Earthquakes and Structures, *Vol. 8, No. 1 (2015) 253-273*
DOI: http://dx.doi.org/10.12989/eas.2015.8.1.253

Simplified finite element modelling of non uniform tall building structures comprising wall and frame assemblies including P-Δ effects

Abdesselem Hichem Belhadj and Sid Ahmed Meftah*

Laboratoire des Structures et Matériaux Avancés dans le Génie Civil et Travaux Publics, Université de Djellali Liabes, BP 89 cité Ben M'hidi Sidi Bel Abbes, Algérie

(Received February 14, 2014, Revised June 10, 2014, Accepted July 5, 2014)

Abstract. The current investigation has been conducted to examine the effect of gravity loads on the seismic responses of the doubly asymmetric, three-dimensional structures comprising walls and frames. The proposed model includes the P-Δ effects induced by the building weight. Based on the variational approach, a 3D finite element with two nodes and six DOF per node including P-Δ effects is formulated. Dynamic and static governing equations are derived for dynamic and buckling analyzes of buildings braced by wall-frame systems. The influences of P-Δ effects and height of the building on tip displacements under Hachinohe earthquake record are investigated through many structural examples.

Keywords: seismic analysis; asymmetric multi-storey buildings; finite element method; P-Δ effects; buckling analysis

1. Introduction

Asymmetric buildings are more vulnerable to earthquake hazards compared to those with symmetric configuration. The recognition of this sensitivity led the researchers to develop analytical and numerical models for dynamic calculation. A general asymmetric tall building may consist of any combination of the different structural forms, such as frames, shear walls and structural cores.

In the analysis of the asymmetric height rise building structure, commercial software such as ETABS (1995) is used. In general, plan stress elements and beam elements are employed to model the shear wall and frames in the analysis of this kind of building structure. Therefore, it is necessary to use a refined finite element model for an accurate analysis of the wall-frame asymmetric tall building structure. But it would be inefficient to subdivide the entire building structure into an finer mesh with a large number of elements because of the tremendous amount of analysis time and computer memory cost.

To avoid with these difficulties, the most common method of analyzing frame-shear wall system adopts the replacement of the original structure by an equivalent plan structure, so that available various techniques such as continuum approach can be applied.

*Corresponding author, Ph.D. Student, E-mail: meftahs@yahoo.com

http://www.techno-press.org/?journal=eas&subpage=7 ISSN: 2092-7614 (Print), 2092-7622 (Online)

The most widely used approximate calculations are based on the continuum method, when the stiffened building structures is replaced by a (continuous) beam.

Several authors applied the continuum models for static analysis of building structures stiffened by one or several lateral load-resisting systems, (Rutenberg *et al*. 1975, Hoenderkamp 2001, 2002). Over the years, the method was extended to eigenvalue problem, that deals with free vibration and buckling analyzes (Balendra *et al.* 1983, Rutenberg *et al.* 1977, Zalka 2001, 2003, Kuang et *al.* 2004, Meftah *et al.* 2008). More recently the spectral seismic calculation was performed by Tarjan *et al.* (2004), Meftah *et al.* (2007). In all of these works, the analyzes were limited to finding static and dynamic characteristics of building structures with constant properties along their height.

Quanfeng *et al.* (1999) presented the transfer matrix method for seismic analysis of tall frame shear wall systems having stepped cross sections.

The most recent contributions are made by Rafezy *et al.* (2008, 2009). The authors presented a simple and accurate numerical model for free vibration analysis of asymmetric tall buildings with variable cross sections.

It is well established that asymmetric buildings exhibit coupled lateral-torsional movements when subjected to earthquake ground excitations. Currently, this coupling effect lead to significant deflections, and thus, the P-Δ effects should be considered in the structural analyzes.

For many years, the P-Δ effects are subjected to study and concern to structural engineers. Ruge (1934) examined the influence of the column weight on the response of simple elastic structures. Jennings *et al*. (1968) worked on the effects of gravity loads on inelastic structural responses. Goel (1969), Andrew (1977) have suggested that, by increasing stiffness of the structure and limiting its drift, the influences of P-Δ effects may be ignored in multi-degree -of freedom systems.

Sivakumaran *et al.* (1994) have formulated a method for seismic analysis of uniform multi-storey buildings by considering the soil-structure interactions and P-Δ effects.

Tjondro *et al.* (1992) have studied the level of significance of the P-Δ effects expressed in terms of stability indices, drift indices and the ratio of base shear to total mass.

Pauly (1978) studied the effects of P-Δ moments on the inelastic dynamic frame responses of reinforced concrete structures.

Carr *et al*. (1980), using a dynamic time-history analysis for inelastic frame structures, investigated the response of several concrete frames with different stiffness properties and strength.

For many years, building codes over the world ignored the influences of the P-Δ effects in the dynamic analysis of tall buildings. Probably due to their complexity. Although, the ASCE 7-05 (2005) recommended the nonlinear static analysis in order to provide the results of the global pushover analysis, in which, the gravity loads are applied to the mathematical model of the structure. In Eurocode 8 (2003) a simplified approach is proposed. This approach is based on the use of the inter-storey drift sensitivity coefficient as function of the design behaviour factor. This procedure may lead to unrealistic sections of the structural members or, more often the impossibility to consider the P-Δ effects by mean of the simplified method, as suggested by the code provisions.

Recently Adam *et al.* (2012) treat rigorously the role of P-Δ effects on the collapse capacity of the single degree of freedom systems. Black (2011) quantified the role of P-Δ effects on reducing the stiffness and strength of steel frame structures.

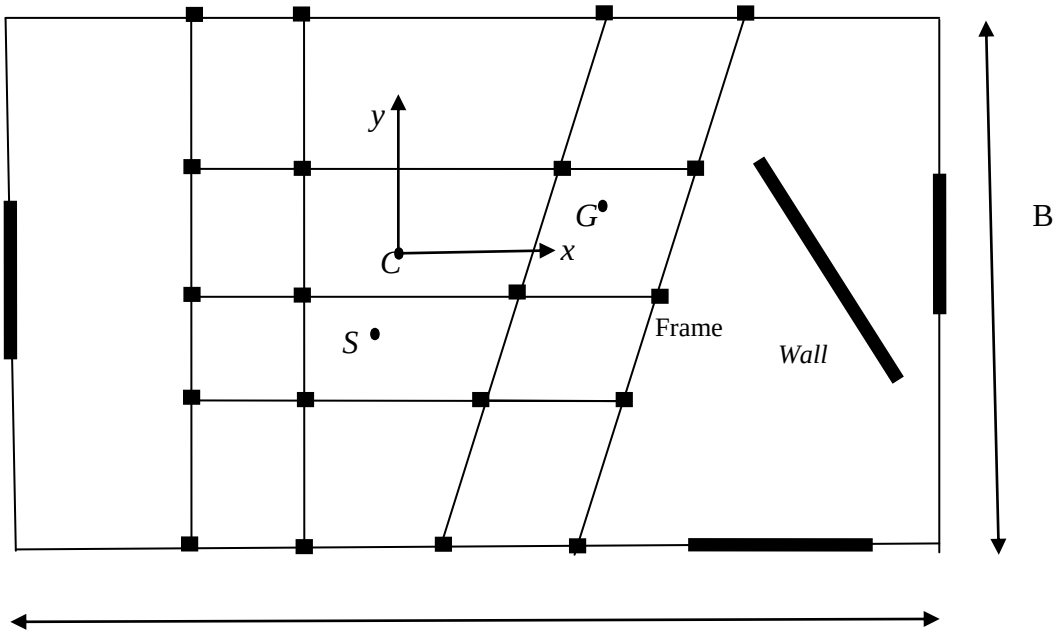

Fig. 1 Floor plan of asymmetric wall-frame building

Although the subject of P-Δ effects on seismic analysis of tall buildings is an old one, the investigations of these effects were limited to regular buildings. Irregularities in geometry and loads are not considered.

To our best Knowledge, there is not work available in the literature aimed at developing a simple finite element which can be used for seismic analysis of stepped frame-wall asymmetric tall buildings including P-Δ effects.

Based on the variational approach, one-dimensional finite element formulation is presented for dynamic analysis of irregular tall buildings braced by frame-shear wall systems. The proposed element has two nodes and six DOF per node including warping effect. The P-Δ effects are described through the geometric stiffness matrix terms. This enlarges the possibilities of solution for more general types of structures, like those with variable geometry or loading without any further difficulty.

This study has proved to be useful for understanding how the P-Δ effects decrease the natural frequencies. Thus, an accurate assessment of tip displacements of asymmetric tall buildings under earthquake excitations can be achieved.

2. Problem statement

The building structure considered comprises frames and shear walls as shown in Fig. 1. The arrangement of the stiffening system is either symmetrical or arbitrary.

The arrangement of the lateral load-resisting system is identical at each floor. Hence, the offsets of the flexural centre are unchanged along the height of the building.

The classes of building structures considered herein have regular and irregular distribution of stiffness in the vertical plan. Uniform mass distribution represents a building with the same concentrated mass at every storey.

The P-Δ effects induced by the second order overturning moments are considered in this study.

Our aim is to develop simple finite element for an accurate assessment of tip displacements of building structures.

3. Method of analysis

3.1 Basic assumptions of approach

One assumes that the material behaviour is linearly elastic.

The effects of the longitudinal inertia forces are negligible in comparison to the horizontal and torsional inertia forces.

The floors are considered to be rigid in their plan and they transfer only horizontal forces to the lateral load-resisting systems.

In the finite element formulation, the continuum approach is applied.

Consider a complex building with the height H, comprised of frames and shear walls as shown

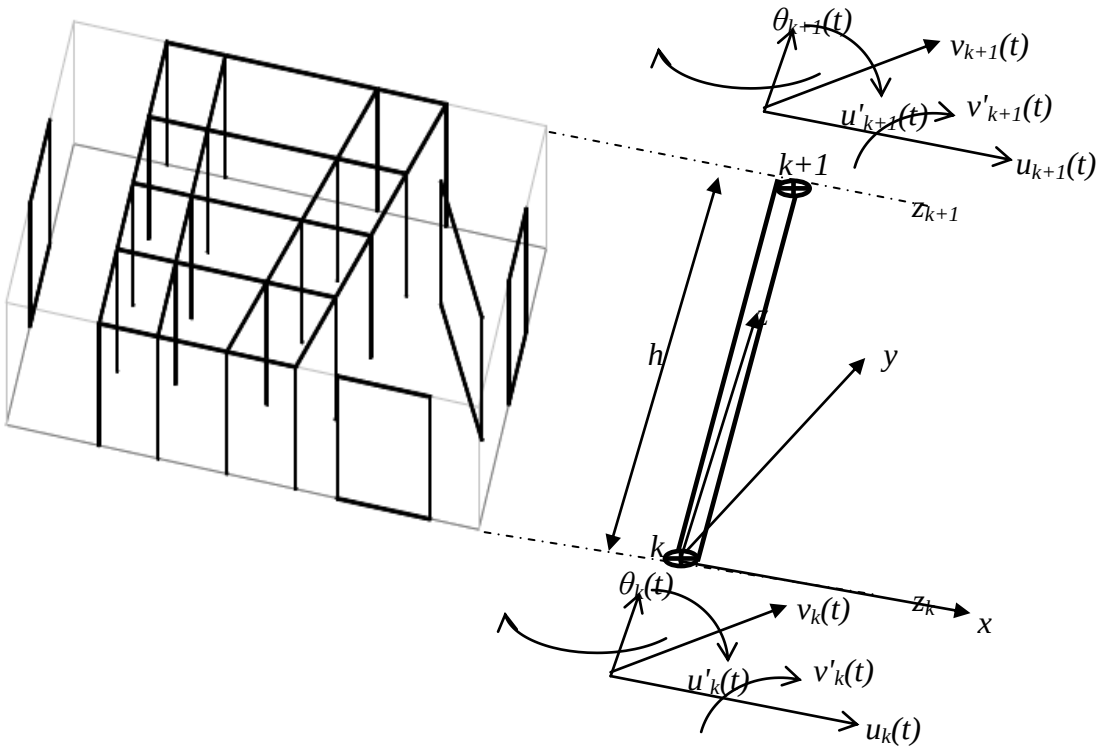

Fig. 2 Finite element formed by cutting the structure through horizontal plane that correspond to the k^{th} and $(k+1)^{th}$ storey level

in Fig. 1. In the analysis, the building structure is dissected into finite elements with two nodes and six DOF per node (Fig. 2). Each finite element describes the structural behaviour between two adjacent storey levels located respectively at z_k and z_{k+1} coordinates as pictured in Fig. 2. Under the action of lateral loads, the flexure-resisting system, such as shear walls are replaced by flexural segment. This segment is positioned at the centre of flexural rigidity *C*, deforming in both flexural lateral directions and warping torsion. Similarly, the shear-resisting structural members such as frames are replaced by an equivalent shear segment. This shear segment is positioned at the centre of shear rigidity $S(x_s,y_s)$, deforming in both lateral shear directions and St. Venant torsion. The vertical *z*-axis is chosen over the structural height and the nodes of the finite elements are located at the centre of flexural rigidity *C*. The coordinates (x_c,y_c) represent the position of geometric centre *G* of the floor plan as shown in Fig. 1.

Each finite element has a uniformly distributed mass *m*, flexural stiffness EI_x, EI_y, and shear stiffness GA_x, GA_y in the *x* and *y* directions respectively, flexural and shear coupling stiffness EI_{xy} and GA_{xy}, warping torsion stiffness EI_ω and St. Venant torsion constant *GJ*.

3.2 Variational formulation

Equilibrium equations for the elastic problem are obtained through the principal of virtual works Bath (996). For a continuum mechanics problem, it reads

$$\delta P^{Int} + \delta P^{Acc} = \delta P^{Ext} + \delta P^{Geom} \tag{1}$$

where δP^{Int} denotes the virtual work of the internal forces; δP^{Ext} the virtual work given by external forces ; δP^{Acc} represents the resulting virtual work put into the system as acceleration and δP^{Geom} is the virtual work related to the geometric nonlinearity, so called P-Δ effects.

The virtual work given by the internal forces is written as

$$\delta P^{Int} = \delta P_b^{Int} + \delta P_s^{Int} \tag{2}$$

In which δP_b^{Int} and δP_s^{Int} denote the virtual works due to bending and shear deformations respectively.

As started previously, the structure assembled may have different rigidity for each floor. Therefore, the structure must be divided along the vertical direction in such way, that the rigidity of each storey element becomes constant. Taking a storey element as the i^{th} element formed by flexural and shear segments as shown in Fig. 2, the bending and shear virtual works are defined as

$$\delta P_b^{Int} = \int_0^h \begin{pmatrix} EI_x \dfrac{\partial^2 u(z,t)}{\partial z^2} \delta \dfrac{\partial^2 u(z,t)}{\partial z^2} + EI_{xy} \dfrac{\partial^2 u(z,t)}{\partial z^2} \delta \dfrac{\partial^2 v(z,t)}{\partial z^2} + \\ EI_{xy} \dfrac{\partial^2 v(z,t)}{\partial z^2} \delta \dfrac{\partial^2 u(z,t)}{\partial z^2} + \\ EI_y \dfrac{\partial^2 v(z,t)}{\partial z^2} \delta \dfrac{\partial^2 v(z,t)}{\partial z^2} + EI_\omega \dfrac{\partial^2 \theta(z,t)}{\partial z^2} \delta \dfrac{\partial^2 \theta(z,t)}{\partial z^2} \end{pmatrix} dz \tag{3}$$

$$\delta P_s^{Int} = \int_O^h \begin{pmatrix} GA_x \dfrac{\partial(u(z,t)-y_s\theta(z,t))}{\partial z}\,\delta\,\dfrac{\partial\,(u(z,t)-y_s\theta(z,t))}{\partial z} + \\ GA_{xy}\dfrac{\partial\,(u(z,t)-y_s\theta(z,t))}{\partial z}\,\delta\,\dfrac{\partial(v(z,t)+x_s\theta(z,t))}{\partial z} + \\ GA_{xy}\dfrac{\partial\,(v(z,t)+x_s\theta(z,t))}{\partial z}\,\delta\,\dfrac{\partial(u(z,t)-y_s\theta(z,t))}{\partial z} + \\ GA_y\dfrac{\partial\,(v(z,t)+x_s\theta(z,t))}{\partial z}\,\delta\,\dfrac{\partial(v(z,t)+x_s\theta(z,t))}{\partial z} + GJ\,\dfrac{\partial\theta(z,t)}{\partial z}\,\delta\,\dfrac{\partial\,\theta(z,t)}{\partial z} \end{pmatrix} dz \quad (4)$$

where $u(z,t)$ and $v(z,t)$ are the deflections of the centre C in x and y directions respectively, and $\theta(z,t)$ is the angle of rotation of the floor plan about the point C.

h is the height of each finite element, given by

$$h = z_{k+1} - z_k \quad (5)$$

The external work arising from the earthquake is defined by

$$\delta P^{Ext} = m\int_0^h \left(\ddot{S}_x\ \delta(u(z,t)-y_c\theta(z,t)) + \ddot{S}_y\ \delta(v(z,t)+x_c\theta(z,t)) \right) dz \quad (6)$$

$\ddot{S}_x$ and $\ddot{S}_y$ are the earthquake ground accelerations under x and y directions respectively, expressed as

$$\begin{Bmatrix} \ddot{S}_x \\ \ddot{S}_y \end{Bmatrix} = \ddot{S}_g \{l\} \quad (7)$$

where $\ddot{S}_g$ is the ground acceleration and $\{l\}$ is the influence vector, which represents the direction of excitation defined by the angle ξ

$$\{l\} = \begin{Bmatrix} \cos(\xi) \\ \sin(\xi) \end{Bmatrix} \quad (8)$$

The virtual work due to the acceleration movement of the building is written as

$$\delta P^{Acc} = m\int_0^h \begin{pmatrix} (\ddot{u}(z,t) - y_c\,\ddot{\theta}(z,t))\ \ \delta(u(z,t)-y_c\theta(z,t)) + \\ (\ddot{v}(z,t) + x_c\,\ddot{\theta}(z,t))\,\delta\,(v(z,t)+x_c\theta(z,t)) + r^2\ddot{\theta}(z,t)\,\delta\,\theta(z,t) \end{pmatrix} dz \quad (9)$$

($\ddot{}$) denotes second derivatives with respect to time.

In addition to the above virtual works, the second order terms may be considered which account for P-Δ effects. These terms are given by

$$\delta P^{Geom} = \int_0^h w(z) \left(\begin{array}{l} \dfrac{\partial (u(z,t) - y_c \theta(z,t)}{\partial z} \delta \dfrac{\partial (u(z,t) - y_c \theta(z,t)}{\partial z} \\ + \\ \dfrac{\partial (v(z,t) + x_c \theta(z,t)}{\partial z} \delta \dfrac{\partial (v(z,t) + x_c \theta(z,t)}{\partial z} \end{array} \right) dz \tag{10}$$

in the above equation $w(z)$ denotes the weight of the structure at the z position of the i^{th} finite element. Assuming triangular variation according to the z direction, the expression of $w(z)$ is defined as

$$w(z) = mg(H - z_k - z) \tag{11}$$

3.3 Finite element formulation

The finite element discretization is used for Eqs. (3), (4), (6), (9), (10). This study employs three-dimensional finite element bounded by two nodal points. Each node has six degrees of freedom (DOF) which describe the lateral displacements (u_n, v_n) and twist angle θ_n and their derivatives at the nodes. The total set of nodal displacements for the elements are

$$\left\{q^{el}(t)\right\} = \begin{Bmatrix} q_k(t) \\ q_{k+1}(t) \end{Bmatrix} = \left\{u_k(t) \;\; u_k^{'}(t) \;\; v_k(t) \;\; v_k^{'}(t) \;\; \theta_k(t) \;\; \theta_k^{'}(t) \;\; u_{k+1}(t) \;\; u_{k+1}^{'}(t) \;\; v_{k+1}(t) \;\; v_{k+1}^{'}(t) \;\; \theta_{k+1}(t) \;\; \theta_{k+1}^{'}(t)\right\}^T \tag{12}$$

(') denotes the derivatives with respect to z direction. With the classical polynomial shape functions, the displacements field vector may be written as

$$\begin{Bmatrix} u(z) \\ v(z) \\ \theta(z) \end{Bmatrix} = \begin{bmatrix} U(z) \\ V(z) \\ \Phi(z) \end{bmatrix} \left\{q^{el}(t)\right\} \tag{13}$$

$[U(z)]$, $[V(z)]$ and $[\Phi(z)]$ are the shape functions listed in Appendix. Inserting Eq. (13) into Eq. (1) and using Eqs. (3), (4), (6), (9), (10), one obtains the following approximate form of the potential energy for each element

$$\begin{aligned} &\left\{q^{el}(t)\right\}^T \left[K_{el}\right] \delta \left\{q^{el}(t)\right\} - \left\{q^{el}(t)\right\}^T \left[K_{el}{}^{Geom}\right] \delta \left\{q^{el}(t)\right\} + \\ &\frac{\partial^2}{\partial t^2} \left\{q^{el}(t)\right\}^T \left[M_{el}\right] \delta \frac{\partial^2}{\partial t^2} \left\{q^{el}(t)\right\} = \left\{F\right\} \ddot{S}_g \end{aligned} \tag{14}$$

where

$$[K_{el}]=\int_0^h \frac{\partial^2}{\partial z^2}\begin{bmatrix}U(z)\\V(z)\\\Phi(z)\end{bmatrix}[E]\frac{\partial^2}{\partial z^2}\begin{bmatrix}U(z) & V(z) & \Phi(z)\end{bmatrix}dz$$

$$+ \tag{15-a}$$

$$\int_0^h \frac{\partial}{\partial z}\begin{bmatrix}U(z)\\V(z)\\\Phi(z)\end{bmatrix}[G]\frac{\partial}{\partial z}\begin{bmatrix}U(z) & V(z) & \Phi(z)\end{bmatrix}dz$$

$$\left[K^{Geo?}\right]=\int_0^L \frac{\partial^2}{\partial z}\begin{bmatrix}U(z)\\V(z)\\\Phi(z)\end{bmatrix}g[m]\frac{\partial^2}{\partial z^2}\begin{bmatrix}U(z) & V(z) & \Phi(z)\end{bmatrix}dz \tag{15-b}$$

$$[M]=\int_0^h \frac{\partial^2}{\partial t^2}\begin{bmatrix}U(z)\\V(z)\\\Phi(z)\end{bmatrix}[m]\begin{bmatrix}U(z) & V(z) & \Phi(z)\end{bmatrix}dz \tag{15-c}$$

$$\{F\}=\int_0^h [m]\begin{bmatrix}U(z) & V(z) & \Phi(z)\end{bmatrix}dz\ \{l\} \tag{15-d}$$

where [*E*]; [*G*] and [*m*] represent the flexural stiffness, shear stiffness and mass matrices given respectively by

$$[E]=\begin{bmatrix}EI_x & EI_{xy} & 0\\EI_{xy} & EI_y & 0\\0_c & 0 & EI_\omega\end{bmatrix} \tag{16-a}$$

$$[G]=\begin{bmatrix}GA_x & GA_{xy} & -y_s GA_x\\GA_{xy} & GA_y & x_s GA_y\\-y_s GA_x & x_s GA_y & GJ\end{bmatrix} \tag{16-b}$$

$$[m]=\begin{bmatrix}1 & 0 & -y_c\\0 & 1 & x_c\\-y_c & x_c & R^2\end{bmatrix} \tag{16-c}$$

[K_e]; [K^{Geom}]; and [*M*] are respectively, the element stiffness ;geometric and mass matrices.

R is the inertial radius of gyration given in Appendix. In the framework of finite element method, the equilibrium equation is formulated as

$$\sum_{el}\left(\left[K_{el}\right]-w\left[K_{el}{}^{Geom}\right]\right)\{q(t)\}+\sum_{el}\left[C_{el}\right]\dot{q}(t)+\sum_{el}\left[M_{el}\right]\ddot{q}(t)=-\sum_{el}\left[M_{el}\right]\{l\}\ddot{S}_g \tag{17}$$

Σ_{el} denotes the assembling process over basic elements. $[C_e]$ is the element damping matrix.

4. Analysis procedures

4.1 Buckling analysis

Buckling analysis of the general structure shown in Fig. 1 is performed by making the nullity of the masses and damping matrices in Eq. (14), one gets

$$\sum_{el}\left(\left[K_{el}\right]-w\left[K_{el}{}^{Geom}\right]\right)\{q_{el}\} \tag{18}$$

from the above equation the critical weight which can lead to the instability of the whole building structure is determined by solving the equation

$$\left|\sum_{el}\left(\left[K_{el}\right]-w_{cr}\left[K_{el}{}^{Geom}\right]\right)\right|=0 \tag{19}$$

w_{cr} is considered as the ultimate value of the building weight. The building designer must be restricted with this value.

4.2 Free vibration analysis

Free vibration problem of the building structure braced by shear walls and frames in which the P-Δ effects are considered, may be formulated in the same fashion as the buckling problem. Then one solves the standard eigenvalue problem

$$\left|\sum_{el}\left(\left[K_e\right]-\mu\, w_{cr}\left[K_e{}^{Geom}\right]\right)-\omega^2\sum_{el}\left[M\right]\right|=0 \tag{20}$$

in which $\mu=w/w_{cr}\in[0\ 1]$ and ω are respectively the weight ratio and the circular frequency.

4.3 Time-history analysis

In this section, the structures are subjected to time-history analysis using Hachinohe earthquake record Fig. 3. For consistent analysis, the earthquake record is scaled to the peak acceleration of 1.0 g (g=9.81 m/s^2). The dominant frequencies are evaluated by Welch's method (Welch 1967) using fast Fourier transform techniques. These frequencies are in the range of 0.19 to 2.19 Hz

The damping matrix of the structure is assumed to be proportional to the stiffness and mass matrices by the Rayleigh's proportionality factors α_1, α_2 (Chopra 2000) as follows

$$\sum_{el}\left[C\right]=\alpha_1\sum_{el}\left[M\right]+\alpha_2\sum_{el}\left(\left[K\right]-\left[K^{Geom}\right]\right) \tag{21}$$

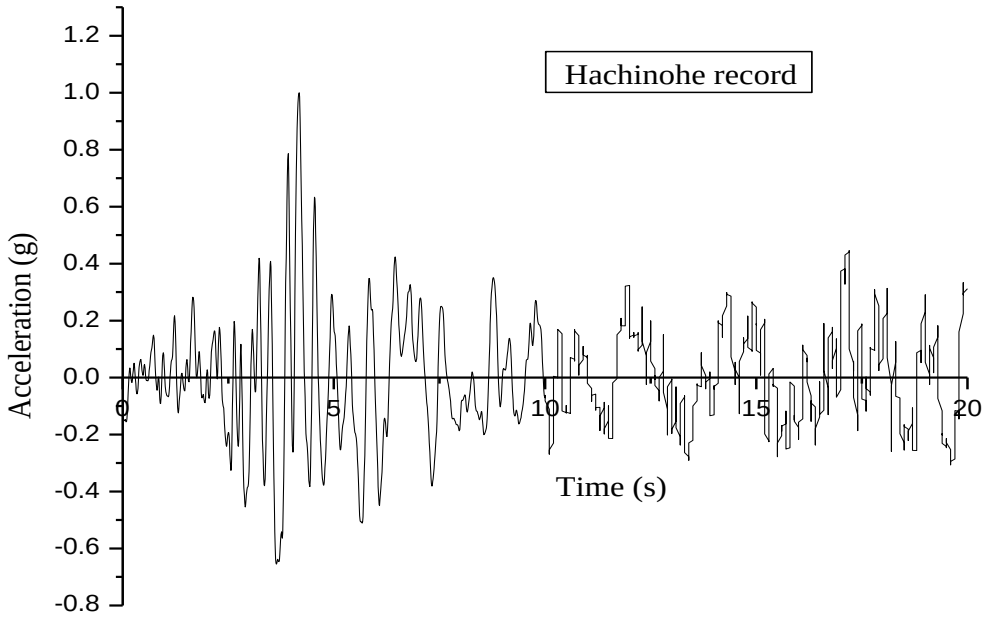

Fig. 3 Hachinohe earthquake record

The proportionality factors α_1, α_2 can be obtained from

$$\alpha_1 = \xi \frac{2\lambda_j \lambda_p}{\lambda_j + \lambda_p} \ , \ \alpha_2 = \xi \frac{2}{\lambda_j + \lambda_p} \tag{22}$$

where λ_j and λ_p are two chosen natural frequencies of the coupled shear wall structures, which are determined by solving the Eq. (20).

The present study is devoted to concrete material, the 1st and 2nd vibration modes are selected, and the viscous damping ξ is fixed to 5% of the critical damping.

Newmark-β step by-step time integration method (Newmark 1959) is employed to get the solution of the dynamic equation, expressed in Eq. (14).

5. Numerical investigation

Results obtained via computer programs prepared in FORTRAN are presented for a variety wall-frame building structures.

5.1 Validation in free vibration analysis

In order to verify the accuracy and the versatility of the proposed method, the free vibrations problem of frame-wall structures of 10, 20, 40 and 60 storey levels proposed by Rafezy *et al.* (2008) is considered. These structures are regrouped into three categories, referring to their floor plans (Fig. 4a, b, c). In all twelve asymmetric structures are studied. A concise description of the

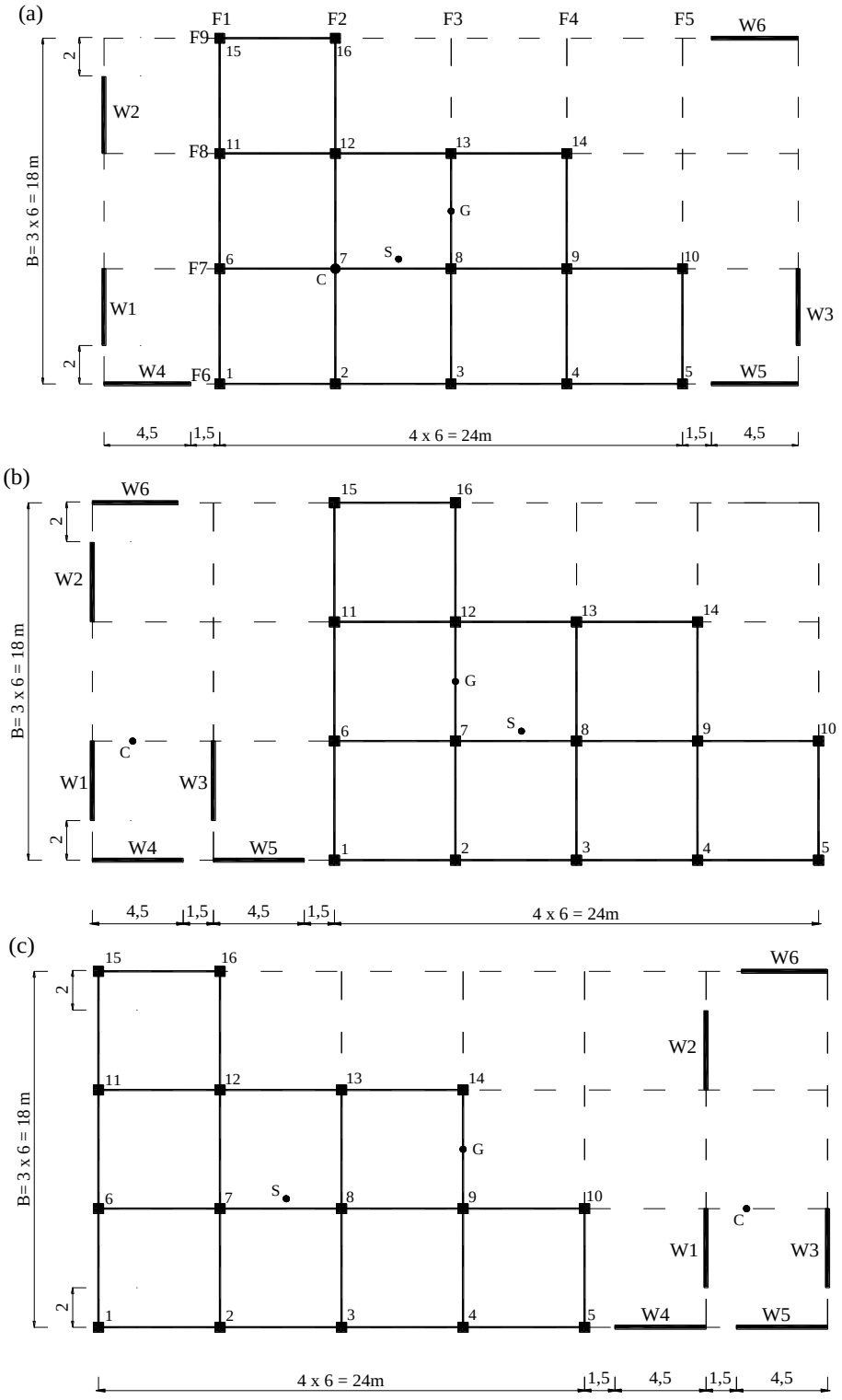

Fig. 4 Floor plan of the considered structures; (a) Floor plan1; (b) Floor plan2; (c) Floor plan3

Table 1a Mechanical properties of the building structures with floor plan of Fig. 4(a)

Building height (storeys)	Floors	Data groups required to define structure properties											
				Coordinate				Flexural and torsion stiffnesses			Shear and torsion stiffnesses		
		m (kg/m)	r_m^2 (m^2)	x_s (m)	y_s (m)	x_c (m)	y_c (m)	EI_x (10^{10} Nm^2)	EI_y (10^{10} Nm^2)	EI_w (10^{12} Nm^4)	GA_x (10^8N)	GA_y (10^8N)	GJ (10^{11} Nm^2)
10	1st to 10th	77760	180	3.273	0.5	6	3	9.113	6.40	24.99	5.647	5.176	0.5591
20	1st to 20th	77760	180	3.273	0.5	6	3	9.113	6.40	24.99	5.647	5.176	0.5591
40	1st to 20th	77760	180	3.273	0.5	6	3	11.39	8.00	31.24	11.290	10.350	1.118
	21st to 40th							9.113	6.40	24.99	5.647	5.176	0.5591
60	1st to 20th	77760	180	3.273	0.5	6	3	13.67	9.60	37.49	22.590	20.710	2.236
	21st to 40th							11.39	8.00	31.24	11.290	10.350	1.118
	41st to 60th							9.113	6.40	24.99	5.647	5.176	0.5591

Table 1b Mechanical properties of the building structures with floor plan of Fig. 4(b)

Building height (storeys)	Floors	Data groups required to define structure properties											
				Coordinate				Flexural and torsion stiffnesses			Shear and torsion stiffnesses		
		m (kg/m)	r_m^2 (m^2)	x_s (m)	y_s (m)	x_c (m)	y_c (m)	EI_x (10^{10} Nm^2)	EI_y (10^{10} Nm^2)	EI_w (10^{12} Nm^4)	GA_x (10^8N)	GA_y (10^8N)	GJ (10^{11} Nm^2)
10	1st to 10th	77760	400	19.273	0.5	16	3	9.113	6.40	7.073	5.647	5.176	2.426
20	1st to 20th	77760	400	19.273	0.5	16	3	9.113	6.40	7.073	5.647	5.176	2.426
40	1st to 20th	77760	400	19.273	0.5	16	3	11.390	8.00	8.841	11.290	10.350	4.853
	21st to 40th							9.113	6.40	7.073	5.647	5.176	2.426
60	1st to 20th	77760	400	19.273	0.5	16	3	13.670	9.60	10.61	22.590	20.710	9.705
	21st to 40th							11.390	8.00	8.841	11.290	10.350	4.853
	41st to 60th							9.113	6.40	7.073	5.647	5.176	2.426

data of these structures is listed in Table 1(a-c).

The buildings of 10 and 20 storeys high are uniform and their properties are unchanged along the height of the structure. But a stepwise change every 20 storeys is considered in the 40 and 60 storey buildings. All storeys are of 3 m height.

Table 1c Mechanical properties of the building structures with floor plan of Fig. 4(c)

Building height (storeys)	Floors	Data groups required to define structure properties											
				Coordinate				Flexural and torsion stiffnesses			Shear and torsion stiffnesses		
		m (kg/m)	r^2_m (m^2)	x_s (m)	y_s (m)	x_c (m)	y_c (m)	EI_x (10^{10} Nm^2)	EI_y (10^{10} Nm^2)	EI_w (10^{12} Nm^4)	GA_x (10^8N)	GA_y (10^8N)	GJ (10^{11} Nm^2)
10	1st to 10th	77760	340	-22.727	0.5	-14	3	9.113	6.40	7.073	5.647	5.176	3.177
20	1st to 20th	77760	340	-22.727	0.5	-14	3	9.113	6.40	7.073	5.647	5.176	3.177
40	1st to 20th	77760	340	-22.727	0.5	-14	3	11.390	8.00	8.841	11.290	10.350	6.355
	21st to 40th							9.113	6.40	7.073	5.647	5.176	3.177
60	1st to 20th	77760	340	-22.727	0.5	-14	3	13.670	9.60	10.61	22.590	20.710	12.71
	21st to 40th							11.390	8.00	8.841	11.290	10.350	6.355
	41st to 60th							9.113	6.40	7.073	5.647	5.176	3.177

Table 2 Comparison of circular frequencies (Hz) of the proposed FEM and Rafezy *et al*. 2008

Frequencies	Floor plan of Fig. 4(a)		Floor plan of Fig. 4(b)		Floor plan of Fig. 4(c)	
	Proposed FEM	Rafezy *et al*.	Proposed FEM	Rafezy *et al*.	Proposed FEM	Rafezy *et al*.
10 Storey buildings						
f_1	0.93752	0.9377	0.88735	0.8875	0.97626	0.9756
f_2	1.10919	1.1085	1.09101	1.0908	1.05811	1.0587
f_3	1.40692	1.4082	1.35033	1.3505	1.34469	1.3452
20 Storey buildings						
f_1	0.36631	0.3664	0.39710	0.3899	0.34730	0.3475
f_2	0.45149	0.4377	0.40402	0.4065	0.44168	0.4415
f_3	0.51242	0.5259	0.50108	0.5013	0.54556	0.5457
40 Storey buildings						
f_1	0.19131	0.1914	0.19945	0.1966	0.16255	0.1627
f_2	0.24488	0.2439	0.23318	0.2385	0.24825	0.2481
f_3	0.27555	0.2767	0.27207	0.2719	0.32170	0.3216
60 Storey buildings						
f_1	0.14803	0.1485	0.14840	0.1487	0.12101	0.1212
f_2	0.19392	0.1937	0.19197	0.1923	0.19717	0.1971
f_3	0.21644	0.2166	0.21633	0.2162	0.26080	0.2607

Table 2 provides the first three frequencies obtained by the proposed FEM without considering P-Δ effects. These are compared to those given by Rafezy *et al.* (2008). The analysis of these data prompts the following comments

• The results given by the proposed FEM agree very well with the results found by Rafezy *et al.* (2008).

• Use of the proposed FEM is economical with respect to consumption of CPU time, data preparation and manipulation efforts. The proposed FEM can be used at the design stages and for final analyzes of the building structures.

5.2 Free vibration analysis with P-Δ effects

To objectively assess the influences of P-Δ effects, free vibrations analysis (including P-Δ effects) is performed. Again, the earlier twenty building structures are considered. Table 3 provides the first three frequencies obtained in both with and without considering P-Δ effects. These frequencies are denoted respectively by $f_i^{P\text{-}\Delta}$ and f_i (*i=1-3*). This set of results leads to the following remarks

The relative differences in frequencies are more pronounced for the 40 and 60 storey buildings compared to those of 10 and 20 storeys. It is shown that the contributions to the higher modes due to the P-Δ effects are negligible. In fact, the most important reduction of 8.12%, corresponding to the fundamental mode is observed in the case of 60 storey building.

Table 3 Comparison of circular frequencies (Hz) with an without considering P-Δ

Frequencies	Floor plan of Fig. 4(a)			Floor plan of Fig. 4(b)			Floor plan of Fig. 4(c)		
	Without P-Δ effects	With P-Δ effects	*Difference* (%)	Without P-Δ effects	With P-Δ effects	*Difference* (%)	With P-Δ effects	Without P-Δ effects	*Difference* (%)
10 Storey buildings									
f_1	0.93752	0.93064	0.74%	0.88735	0.87981	0.86%	0.97626	0.96951	0.70%
f_2	1.10919	1.10334	0.53%	1.09101	1.08509	0.54%	1.05811	1.05199	0.58%
f_3	1.40692	1.40242	0.32%	1.35033	1.34554	0.36%	1.34469	1.33975	0.37%
20 Storey buildings									
f_1	0.36631	0.35732	2.52%	0.39710	0.38821	2.29%	0.34730	0.33793	2.77%
f_2	0.45149	0.44800	0.78%	0.40402	0.39605	2.01%	0.44168	0.43406	1.76%
f_3	0.51242	0.50022	2.44%	0.50108	0.49449	1.33%	0.54556	0.53916	1.19%
40 Storey buildings									
f_1	0.19131	0.18281	4.65%	0.19945	0.18991	5.02%	0.16255	0.15245	6.62%
f_2	0.24488	0.23803	2.88%	0.23318	0.22826	2.15%	0.24825	0.24173	2.70%
f_3	0.27555	0.27001	2.05%	0.27207	0.26616	2.22%	0.32170	0.31663	1.60%
60 Storey buildings									
f_1	0.14803	0.14076	5.17%	0.14840	0.14099	5.25%	0.12101	0.11193	8.12%
f_2	0.19392	0.18833	2.97%	0.19197	0.18661	2.87%	0.19717	0.19179	2.81%
f_3	0.21644	0.21169	2.25%	0.21633	0.21149	2.29%	0.26080	0.25674	1.58%

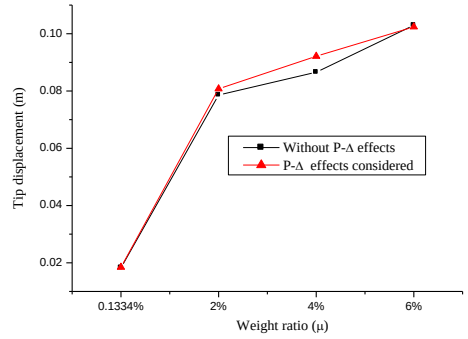

(a)

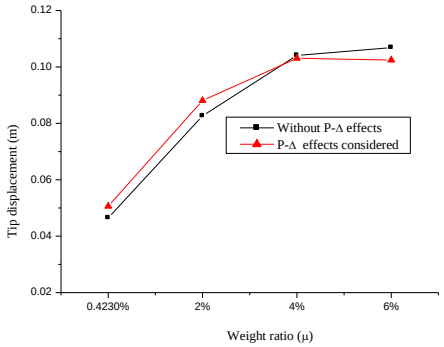

(b)

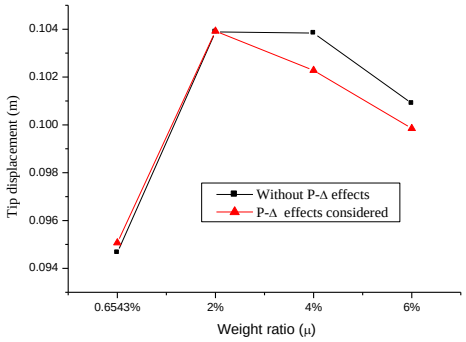

(c)

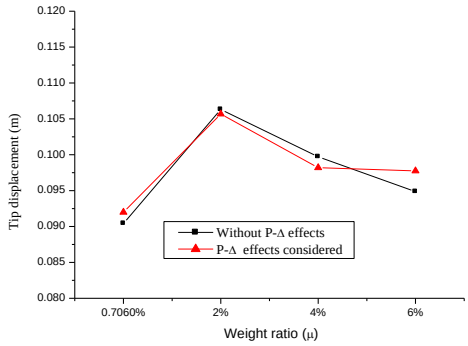

(d)

Fig. 5 P-Δ effects on lateral tip displacements of buildings comprising floor plan1; (a) 10 stories building, (b) 20 stories building, (c) 40 stories building and (d) 60 stories building

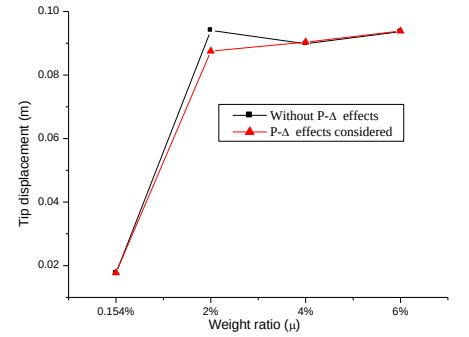

(a)

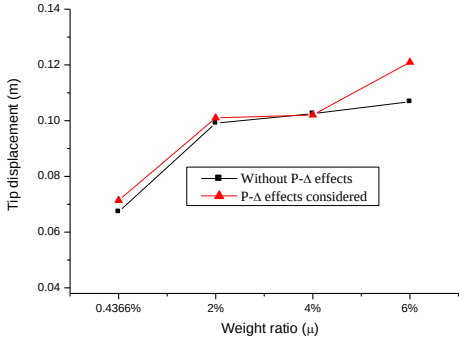

(b)

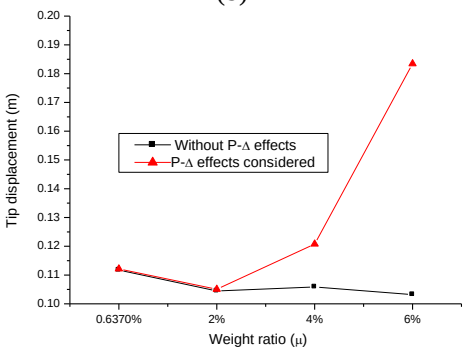

(c)

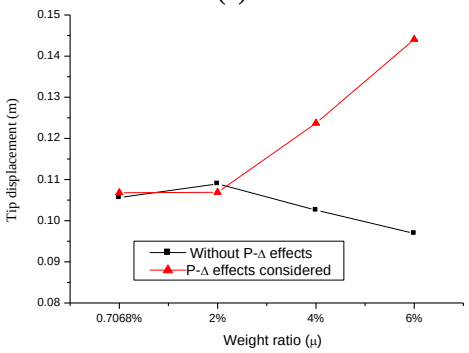

(d)

Fig. 6 P-Δ effects on lateral tip displacements of buildings comprising floor plan2; (a) 10 stories building, (b) 20 stories building, (c) 40 stories building and (d) 60 stories building

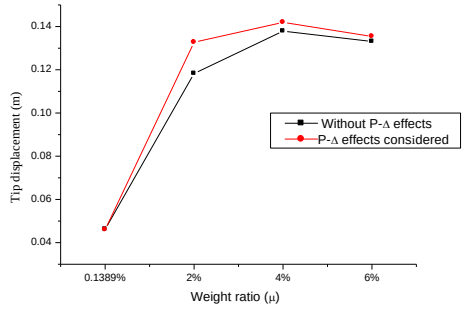

(a)

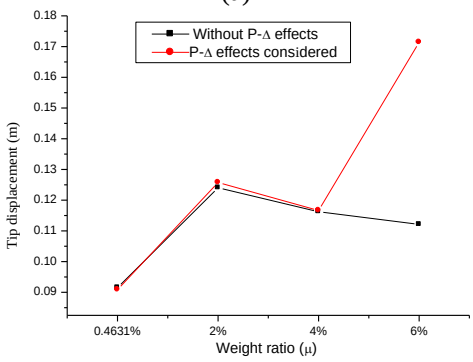

(b)

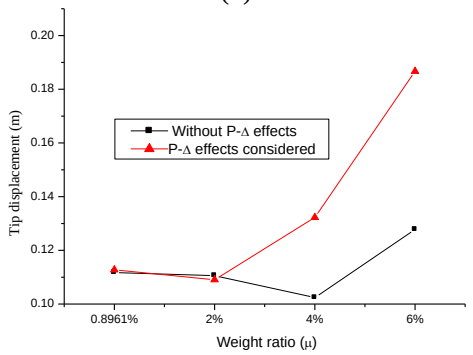

(c)

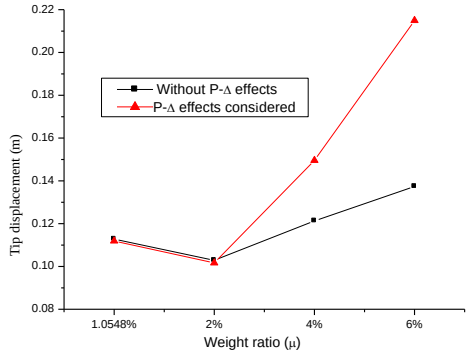

(d)

Fig. 7 P-Δ effects on lateral tip displacements of buildings comprising floor plan1 ; (a) 10 stories building, (b) 20 stories building, (c) 40 stories building and (d) 60 stories building

5.3 Tip deflections under seismic loading

The results for the twelve asymmetric buildings under Hachinohe earthquake record are presented below. The purpose of this study is to illustrate how the P-Δ effects influence the tip deflections under Hachinohe earthquake record. For this goal, The seismic is considered in the *x* direction. Due to torsional rotation of the building, a much larger displacement is experienced at the end of the structure rather than at the centre of mass *G*.

Figs. 5-8 compare the peak values of the lateral displacement variations with respect to the weight ratio μ. From these figures, the P-Δ effects yield, substantial increases on lateral tip deflections of tall buildings.

Fig. 5(a)-(d) illustrate the variation of the tip displacements according to the weight ratio μ expected by the structures of the floor plan of Fig. 4(a). One remark, that for all buildings, the P-Δ effects have no significant influences on tip deflections. A moderated increasing of 9 % is reported for 20 storey building with μ=6% (Fig. 5(b)).

The influences of on the tip displacements for buildings referring to floor plan of Fig. 4(b) are pictured in Fig. 6(a)-(d). From these figures one finds that the contributions to the tip displacements due to P-Δ effects are negligible in the case of 10 and 20 storey buildings. For instance, moderate amplification of 13.3% is reached for 20 storey building with μ=6%.

Contrary, in the cases of 40 and 60 storey buildings (Fig. 6(c), (d)), significant effects are reported. The highest amplification of 78% is achieved by 40 storey building with μ=6% .This was followed by 60 storey building with a tip displacement amplification of 49%.

Fig. 7(a)-(d) report the influences of P-Δ effects on tip displacement of the building structures corresponding to the floor plan of Fig. 4(c). From these figures, it is worth noting that the important effect is achieved in the case of the 60 storey building with a tip deflection amplification of 26.5% for μ=6%, whereas, the lateral stability of the 40 storey building has not been significantly affected by the gravity loads with a moderate tip displacement amplification of 10%. It is needless to say that for 10 and 20 storey buildings (Fig. 7(a), (b)), negligible contributions of P-Δ effects are observed.

The results demonstrated the importance of considering P-Δ effects in the order to provide good estimation of the tip deflections of tall buildings. The outcome of this study will find application in structural buildings by increasing their structural performances to withstand earthquakes without collapsing and without incurring major damages.

This study demonstrated the feasibility of considering P-Δ effects to predict seismic responses of tall buildings. As the natural frequencies of the structural models of 10 and 20 stories are within the frequency range of the dominant modes of the Hachinohe earthquake, this study treated resonant vibrations. It is probably due to this reason that, there are no particular amplification in the seismic responses with respect to P-Δ effects.

6. Conclusions

An efficient finite element model for dynamic analysis of building structures braced by shear walls and frames including P-Δ effects is proposed. The 3D finite element is formulated for dynamic calculation of the doubly asymmetric, three dimensional multi-bay, multi-storey, wall-frame structures. The accuracy and the efficiency of the proposed method were investigated by performing analyses of example structures.

The major conclusions of this study are summarized as bellow

• The main advantage of the proposed approach consists of the drastic reduction of computational effort with respect to the classical FEMs. In fact, the convergence tests confirm that the proposed finite element with a small number of DOF yield accurate results compared to the classical finite elements based on mesh refinements.

• The results indicate that P-Δ effects decrease the flexibility of the building structure also affecting the natural frequencies of the first mode of vibration of the tall building structures with 40 and 60 storey levels.

• The P-Δ effects are quit conservative and only a small influence on the tip lateral displacements was shown for 10 and 20 storey buildings under Hachenohe earthquake.

• In this study, focus has been on the weight ratio μ which refers to the gravity loads. The contribution of this parameter led to a significant influence on the tip displacement amplification.

• This study was demonstrated the difficulty to predict the tip displacement amplification due to the P-Δ effects. It was commonly stated that the deflections are strongly dominated by the range of dominant frequencies of the input earthquake record as a source of resonance effect.

References

Adam, C. and Jager, C. (2013), "Simplified collapse capacity of earthquake excited regular frame structures vulnerable to P-delta", *Eng. Struct*., **44,** 159-173**.**

American Society of Civil Engineering (2005), "Minimum design loads for buildings and other structures", ASCE/SEI 7-05.

Andrews, A.L. (1977), "Slenderness effects in earthquake engineering frames", *B. NZ Natl. Soc. Earthq. Eng*., **10,** 154-158.

Balendra, T., Chan, W.T. and Lee, S.L. (1983), "Vibration of asymmetric building-foundation systems", *J. Mech. Eng*., **109,** 430-449.

Bathe, K.J. (1996), *Finite Element Procedures*, Prentice-Hall, Inc, New Jersey.

Black, E.F. (2011), "Use of stability coefficients for evaluating the P-Δ effect in regular steel moment resisting frames", *Eng. Struct*., **33**, 1205-1216.

Carr, A.J. and Moss, P.J. (1980), "The effects of large displacements on the earthquake response of tall concrete frame structures", *B. NZ Natl. Soc. Earthq. Eng*., **13**(4), 317-328.

Chopra, A.K. (2000), *Dynamic of structures theory and applications to earthquake engineering*, Prentice Halle, New Jersey.

Eorocode 8 (2003), "Design of structures for earthquake resistance", European committee for standardisation.

Goel, S.C. (1969), "P-δ and axial column deformation in a seismic frames", *J. Struct. Div*.**, 95**, 1693-711.

Hoenderkamp, J.C.D. (2001), "Elastic analysis of asymmetric tall building structures", *Struct. Des. Tall Build*., **10**, 245-261.

Hoenderkamp, J.C.D. (2002), "Simplified analysis of asymmetric High-rise structures with cores", *Struct. Des. Tall Build*., **11**, 93-107.

Jennings, P.C. and Husid, R. (1968), "Collapse of yielding structures during earthquakes", *J. Eng. Mech. Div*., **94**, 1045-1065.

Kuang, J.S. and NG, S.C. (2004), "Coupled vibration of tall building structures", *Struct. Des. Tall Spec. Build*., **13**, 291-303.

Meftah, S.A., Tounsi, A. and Adda Bedia, A. (2007), "A simplified approach for seismic calculation of a tall building braced by shear walls and thin-walled open section structures", *Eng. Struct*., **29**, 2579-2585.

Meftah, S.A. and Tounsi, A. (2008), "Vibration characteristics of tall buildings braced by shear walls and thin-walled open section structures", *Struct. Des. Tall Spec. Build*., **17**, 203-216.

Newmark, N.M. (1959), "A method of computation for structural dynamics", *J. Eng. Mech. Div*., **85**, 67-94.
Paulay, T. (1978), "A consideration of P-delta effects in ductile reinforced concrete frames", *B. NZ Natl. Soc. Earthq. Eng*., **11**(3), 151-160.
Quanfeng, W., Lingyun, W. and Qiangsheng, L. (1999), "Seismic response of stepped frame-shear wall structures by using numerical method", *Comput. Method. Appl. M. Eng*., **173**, 31-39.
Rafezy, B. and Howson, W.P. (2008), "Vibration analysis of doubly asymmetric, three dimensional structures comprising wall and frame assemblies with variable cross-section", *J. Sound Vib*., **318**, 247-266.
Rafezy, B. and Howson, W.P. (2009), "Coupled lateral-torsion frequencies of asymmetric, three-dimensional structures comprising shear-wall and core assemblies with stepwise", *Eng. Struct.*, **31**, 1903-1915.
Ruge, A.C. (1934), "The determination of earthquake stresses in elastic structures by means of models", *B. Seismol. Soc. Am*., **24**.
Rutenberg, A. and Heidebrecht, A.C. (1975), "Approximate analysis of asymmetric wall-frame structures", *Building Science*., **10**, 27-35.
Rutenberg, A., Tso, W.K. and Heidebrecht, A.C. (1977), "Dynamic properties of asymmetric wall-frame structures", *Earthq. Eng. Struct. D*., **5**, 41-51.
Sivakumaran, K.S. and Balandra, T. (1994), "Seismic analysis of asymmetric multistorey buildings including foundation interaction and P-Δ effects", *Eng. Struct***., 16**, 609-624.
Tarjan, G. and Kollar, P.L. (2004), "Approximate analysis of building structures with identical stories subjected to earthquakes", *Int. J. S. Struct*., **41,** 1411-1433.
Tjondro, J.A., Moss, P.J. and Carr, J. (1992), "Seismic P-δ effects in medium height moment resisting steel frames", *Eng. Struct*., **14**(2), 75-90.
Welch, P.D. (1967), "The use of fast Fournier transform for the estimation of power spectra; a method based on time averaging aver short modified periodograms", *IEEE. T. Audio Electroacoust*., **15**(2), 70-703.
Zalka, K.A. (2001), "A simplified method for the calculation of the natural frequencies of wall-frame buildings", *Eng. Struct*., **23**(12), 1544-1555
Zalka, K.A. (2003), "A hand method for predicting the stability for regular buildings, using frequency measurements", *Struct. Des. Tall Build*., **12**, 273-281.

IT

Appendix

The shape functions used in section 3 are defined as:

$$\begin{bmatrix} u(z) \\ v(z) \\ \theta(z) \end{bmatrix} = \begin{bmatrix} U(z) \\ V(z) \\ \Phi(z) \end{bmatrix} \begin{bmatrix} q_k \\ q_{k+1} \end{bmatrix}$$

where

$$[U] = [N_1(\xi) \quad N_2(\xi) \quad 0 \quad 0 \quad 0 \quad 0 \quad N_3(\xi) \quad N_4(\xi) \quad 0 \quad 0 \quad 0 \quad 0];$$
$$[V] = [0 \quad 0 \quad N_1(\xi) \quad N_2(\xi) \quad 0 \quad 0 \quad 0 \quad 0 \quad N_3(\xi) \quad N_4(\xi) \quad 0 \quad 0];$$
$$[\Phi] = [0 \quad 0 \quad 0 \quad 0 \quad N_1(\xi) \quad N_2(\xi) \quad 0 \quad 0 \quad 0 \quad 0 \quad N_3(\xi) \quad N_4(\xi)];$$

and

The linear interpolation functions $N_1(\xi)$;$N_2(\xi)$; $N_3(\xi)$ and $N_4(\xi)$ are given by:

$$N_1(\xi) = (1 - 3\xi^2 + 2\xi^3) \ ;$$
$$N_2(\xi) = h(1 - 2\xi^2 + \xi^3);$$
$$N_3(\xi) = (3\xi^2 - 2\xi^3);$$
$$N_4(\xi) = h(-\xi^2 + \xi^3)$$

where

$$\xi = \frac{z}{h}$$

For buildings of rectangular plan-shape (Lx B) and subjected to a uniformly distributed mass at floor levels, the radius of gyration is obtained from

$$R = \sqrt{\frac{L^2 + B^2}{12} + x_C^2 + y_C^2}$$